SUPPLEMENTARY MATERIALS

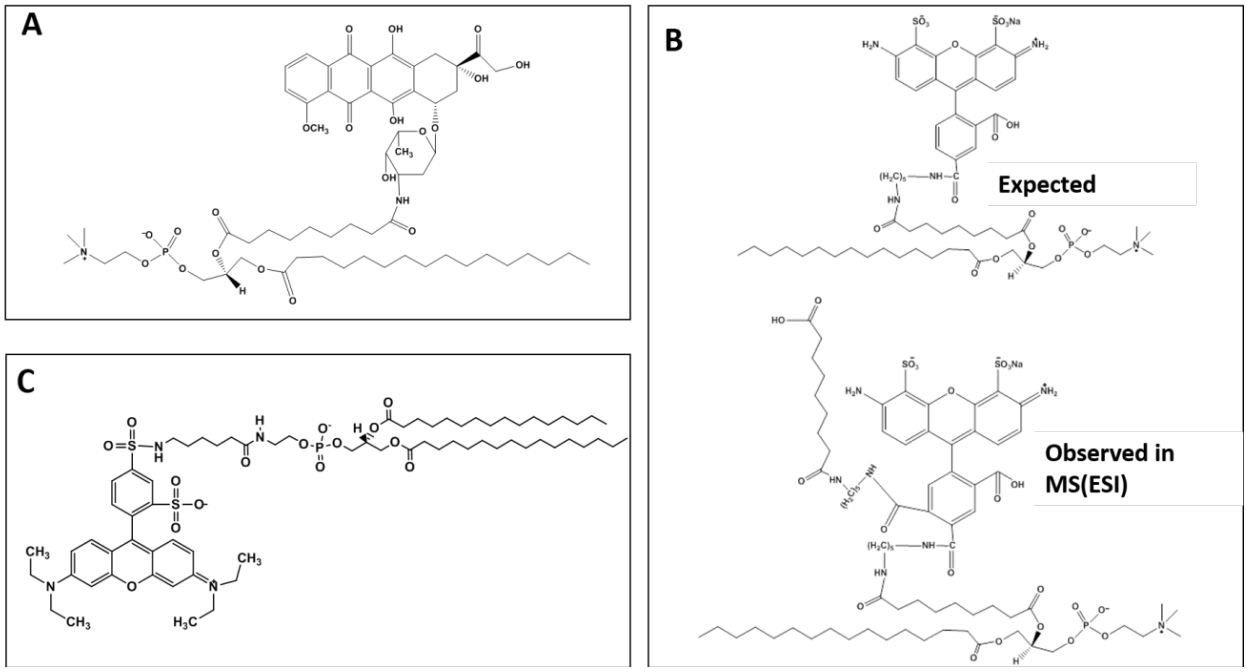

Figure S1: Chemical structures and characterization for Doxorubicin PD, AF488-PD and PE-Rhodamine. (A). Chemical structure of doxorubicin prodrug as described in the methods. Chemical Formula: C60H91N2O20P, ESI-MS M+H+ Cal. 1190.63, exp.1191.6 (Shimadzu LCMS 2010A (Kyoto, Japan). (B). Chemical structure of AlexaFluor™-488-prodrug (AF488-PD) as described in methods. The structure produced in high purity because the purportedly high purity starting materials, AF-488 dye and Paz-PC, were both unexpectedly impure as purchased and received. The Paz-PC, synthesized by NOF America from the lysophosphatidylcholine backbone and the addition of nonanedioic acid at Sn2 contained significant free nonanedioic acid. AlexaFluor™-488 cadaverine purchased from Thermo Fisher Scientific presented two N-(5-aminopentyl)formamide arms instead of one on the benzyl ring. As a consequence, the free nonanedioic acid also coupled to the extra N-(5-aminopentyl)formamide to create a second hydrophobic anchor. Synthesis of this compound into lipid membranes was unaffected and it was used as surrogate biomarker for single-molecule tracking. The final chemical formula was $C_{74}H_{113}N_7NaO_{23}PS_2+2H^+$, ESI-MS $M+H^+$ Cal. 793, exp.793.85 (Shimadzu LCMS 2010A (Kyoto, Japan). (C). Chemical structure of Rhodamine-phosphatidylethanolamine (PE-Rhodamine, Avanti Polar Lipids). It was previously used by Partlow et al. [1].

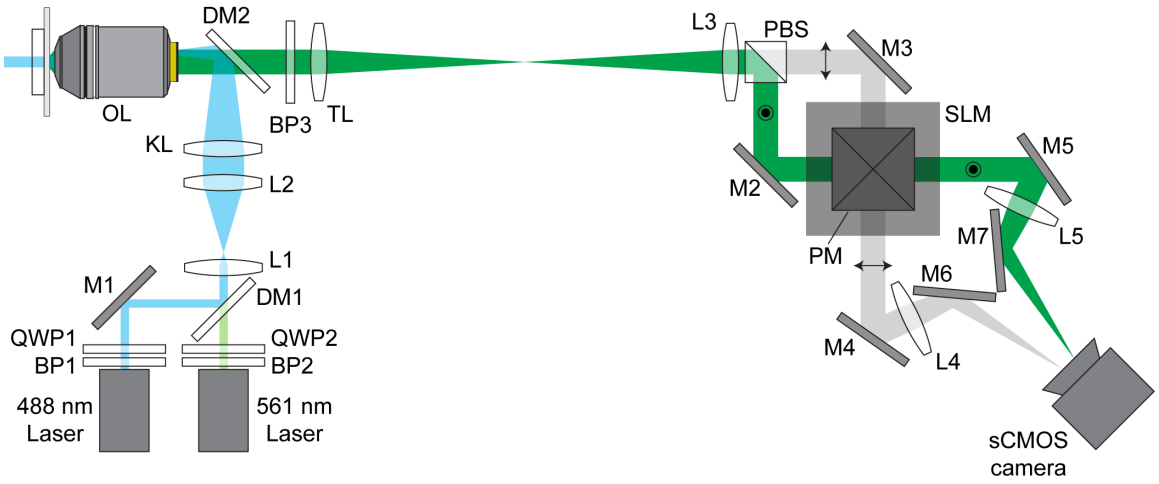

Figure S2. Schematic of imaging system used for single-molecule super-resolution fluorescence imaging. Only one channel of the polarized images was captured and used. BP1-3, bandpass filters; QWP1-2, quarter wave plates; M1-7, mirrors; DM1-2, dichroic mirrors; L1-5, lenses; KL, wide-field lenses; OL, objective lens; TL, tube lenses; PM, pyramidal mirror; PBS, polarizing beam splitter; SLM, spatial light modulator.

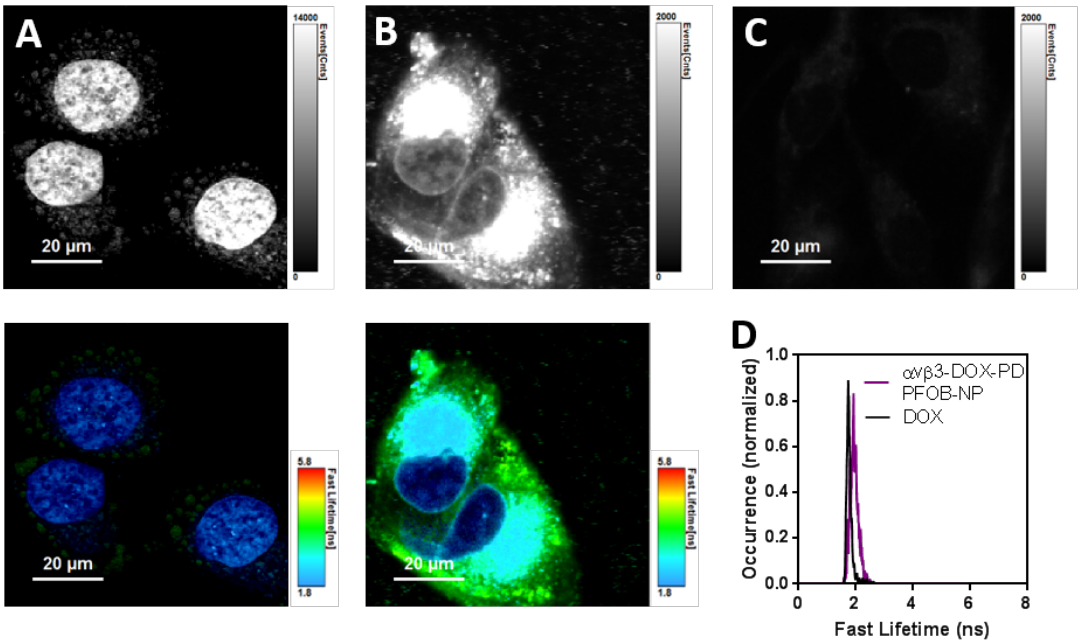

Figure S3: Images of C-32 melanoma cells treated with DOX and $\alpha_v\beta_3$-DOX-PD PFOB-NPs for 1 h. DOX treated cells (A: intensity (top), fast lifetime (bottom)) exhibit strong nuclear signal while the later showed strong fluorescence throughput (B: intensity (top), fast lifetime (bottom), and the untreated cells showed minimal background signal (C (intensity). Cell nuclei in both groups showed similar fast lifetime distribution as shown by the color-coded images and lifetime histogram (D), suggesting that DOX liberated from lipid prodrug retained the same dsDNA binding character as the native compound.

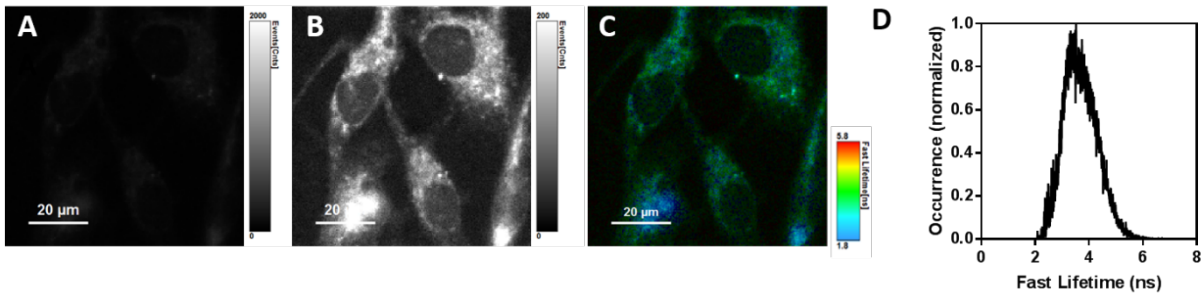

Figure S4: Under the imaging conditions, untreated C-32 cells gave minimal background signal due to cell auto fluorescence and backscattering of excitation laser (A). This signal could be visualized on changing the intensity scale from 0-2000 to 0-200 events (B), and contributed <10% of real fluorescence signal under these conditions. Lifetime of this signal was broadly spread with an average of around ~ 3.5 ns as shown in the histogram (C, D).

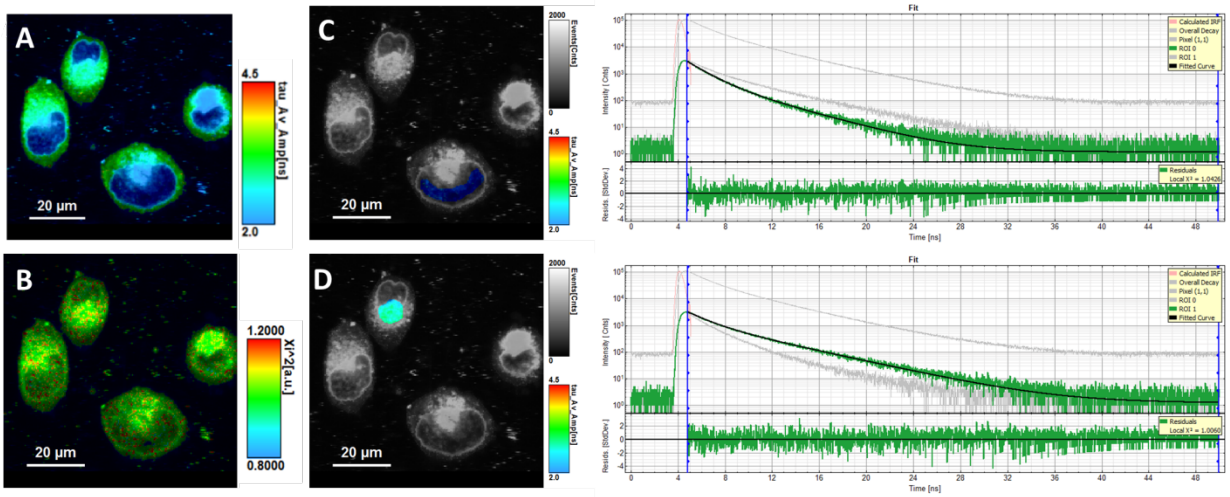

Figure S5: Representative fluorescence lifetime image analysis of C-32 cells treated with $\alpha_v\beta_3$-DOX-PD PFOB-NPs as shown in Figure 4 of main text. The average lifetime image obtained after pixel-by-pixel fit of decay using a bi-exponential decay model (A). The corresponding image displaying the chi-square values obtained shows goodness of fit (A). Nuclear region of interest (C, left) and corresponding fluorescence decay with its bi-exponential fit (C, right, $\chi 2$=1.04). Similar analysis is shown for a region of interest corresponding to the bright perinuclear pace, $\chi 2$ =1.06. (D, left and right)

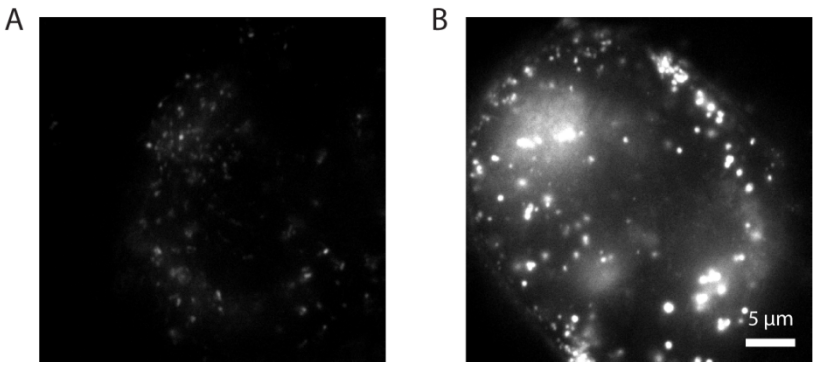

Figure S6. Images of (A) autofluorescence from an untreated 2F2B cell and (B) a 2F2B cell after incubation with 4.0 µg/mL AF488-PD at 37 ºC for 12 hours.

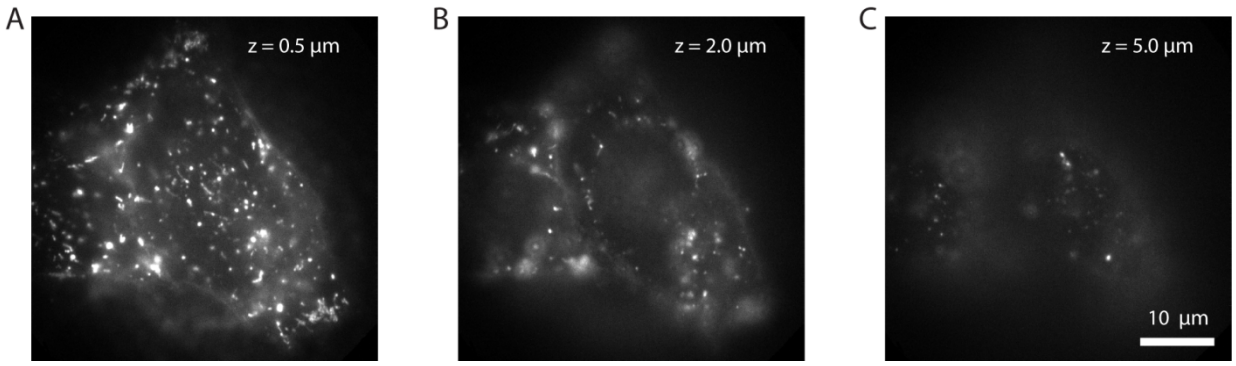

Figure S7. Images of a 2F2B cell at different z heights (0.5, 2.0, 5.0 µm) above the coverslip after incubation with 1.4 µM PE-rhodamine at 37 ºC for 1 hour.

Video S1. Video clip showing the single-molecule fluorescence images of AF488-PD molecules on a 2F2B cell within the same field of view as in Figure 5B in the main text. The trajectory from 0.55 to 4.00 s indicates the diffusive path of a single AF488-PD molecule on the cell membrane (see also, Figure 5B, inset (ii) in the main text).

REFERENCES

1. Partlow KC, Lanza GM, Wickline SA. Exploiting lipid raft transport with membrane targeted nanoparticles: a strategy for cytosolic drug delivery. Biomaterials. 2008; 29: 3367-75.